Core-Shell Strain Structure of Zeolite Microcrystals

Wonsuk Cha[1], Nak Cheon Jeong[2], Sanghoon Song[3], Hyun-jun Park[1], Tung Cao Thanh Pham[2], Ross Harder[4], Bobae Lim[5], Gang Xiong[6], Docheon Ahn[7], Ian McNulty[4], Jungho Kim[3,5], Kyung Byung Yoon[2,3], Ian K. Robinson[6,8], Hyunjung Kim[1,3†]

[1]Department of Physics, Sogang University, Seoul 121-742, Korea
[2]Department of Chemistry, Sogang University, Seoul 121-742, Korea
[3]Interdisciplinary Program of Integrated Biotechnology, Sogang University, Seoul 121-742, Korea
[4]Advanced Photon Source, Argonne National Laboratory, Argonne, IL 60439, USA
[5]Department of Life Sciences, Sogang University, Seoul 121-742, Korea
[6]London Centre for Nanotechnology, University College, London WC1H 0AH, UK
[7]Pohang Accelerator Laboratory, Pohang 790-784, Korea
[8]Research Complex at Harwell, Didcot, Oxford OX11 0DE, UK
[†]e-mail: hkim@sogang.ac.kr

Zeolites are crystalline aluminosilicate minerals featuring a network of 0.3-1.5 nm wide pores, used in industry as catalysts for hydrocarbon interconversion, ion exchangers, molecular sieves, and adsorbents[1]. For improved applications, it is highly useful to study the distribution of internal local strains because they sensitively affect the rates of adsorption and diffusion of guest molecules within zeolites[2,3]. Here, we report the observation of an unusual "triangular" deformation field distribution in ZSM-5 zeolites by coherent x-ray diffraction imaging[4], showing the presence of a strain within the crystal arising from the heterogeneous core-shell structure, which is supported by finite element model calculation and confirmed by fluorescence measurement. The shell is composed of H-ZSM-5 with intrinsic negative thermal expansion[5] while the core exhibits different thermal expansion behavior due to the presence of organic template residues, which usually remain when the starting materials are insufficiently calcined. (142 words) Engineering such strain effects could have major impact on the design of future catalysts.

[needs a concluding sentence describing the broader significance of the work.]

1. **The strain field distribution with such small traces was only possible to be detected by CDI.**

2. **Thus the number density and the distribution pattern of the guests within zeolite crystals are two important factors that sensitively affect the diffusion dynamics of guests and the shape selectivity of zeolite pores.**
3. **These observed structures could explain the loss of efficiency due to effective volume reduction.(?)**

Zeolites, having subnanometer-scale pores lined with chemically active surfaces, are widely used as catalysts, sorbents, ion exchangers, molecular separation membranes[6-14], membrane reactors[15], and many others[1]. Although each zeolite has well-defined pore sizes and shapes, they could undergo a significant degree of distortion if the zeolite crystal is situated under a strongly strained condition. If this happens the rates of adsorption of molecules into the zeolite channels, subsequent diffusion within the channels, and desorption from the channels to the exteriors will be greatly altered. Although structural changes of crystals have often been measured by x-ray and neutron powder diffraction[16,17], such diffraction techniques can only measure the averaged variation of the whole, without finely discriminating the local structural variations within the crystals such as the difference between the core and outermost parts of the crystals. In this respect, elucidation of the three-dimensional patterns, degrees, and the causes of the strains will greatly help to explain the observed activities of zeolites during their applications and to design appropriate conditions to improve activities.

ZSM-5 is an aluminosilicate zeolite having 5.5 × 5.1 $Å^2$ sized elliptical channels running along the *a*-axis in a sinusoidal manner and 5.6 × 5.3 $Å^2$ sized elliptical channels running straight along the *b*-axis. This zeolite is usually synthesized from the gels containing a Si source, an Al source, tetrapropylammonium hydroxide (TPAOH), a base, and water. The use of TPAOH is necessary because the TPA^+ ions act as the structure-directing agents. As a result, these organic ions become entrapped at the intersections between the sinusoidal and straight channels, thereby blocking the channels[18]. Therefore, they must be removed from ZSM-5 crystals by calcination[19] (usually by heating at 450-550°C for several hours under the flowing oxygen or air) before the crystals can be used for catalysis, adsorption, and separation. However, if the zeolite is calcined at lower temperatures or calcined not long enough even at the required temperatures, corks or residual carbon compounds can remain in crystals, thereby still partially blocking the channels.

ZSM-5 crystals have complex temperature-dependent anisotropic thermal expansion coefficients.[5,17,20,21] Accordingly, each crystal undergoes anisotropic thermal expansion during the initial stage and anisotropic thermal contraction during the later stage of calcination, that is, in the 25-150°C and 150-550°C regions, respectively.

In this letter, using ZSM-5 crystals supported on a silicon substrate as model zeolite crystals we have studied the formation of strain within the attached crystals. We now report an unusual internal deformation field distribution in a micrometer-sized crystal of ZSM-5 attached on a silicon substrate along the calcination condition by coherent x-ray diffraction imaging (CDI)[4].

When the crystal dimensions are smaller than the illuminated coherence volume, using coherent x-rays available from a third-generation synchrotron, the scattering from all parts of the sample interferes in the far-field diffraction pattern. The internal deformation of lattice from the ideal structure is imaged as a shifted phase map, arising from the asymmetric part of the x-ray diffraction pattern at each Bragg reflection; the symmetric part can be considered to come from internal electron density of the crystal[4,22-23].

A schematic picture of the geometry in the coherent x-ray diffraction (CXD) experiment along (200) reflection of a ZSM-5 microcrystal measured in nitrogen is shown in Fig. 1a. Typically, CXD patterns are expected to show characteristic Airy ring patterns around the Bragg peak at the center and a vertical streak attributed to its (200) facets[22]. [See Fig. S1 in supplementary information (SI)]. From the diffraction patterns as a function of temperature with different calcination conditions, we have observed a range of patterns between the two extremes shown in Fig. 1b and 1c. Figure 1b shows a diffraction pattern indicating a relatively unstrained state of the crystal, while Fig. 1c exhibits a more distorted diffraction pattern: the shape at the center of Bragg peak is triangular and the fringes are no longer along the crystal axes. The perpendicular section of the three-dimensional diffraction patterns at 90° [in the bottom-right panels in Fig. 1b and 1c for each case] do not show such distorted shape implying that the distortions are mostly confined to the (020) plane of the crystal.

A phase retrieval algorithm was applied to the data to phase the measured diffraction patterns. We used error reduction and hybrid input-output methods[24] with the restricted phase (because the phases are not changed beyond that range) and with finite supports as the real-space constraints. Once phased, the three-dimensional data

were inverted to real space by Fourier transformation and a coordinate transformation. Further details are given in SI. In Fig. 1d, a 37.5% isosurface of resulting density of the three-dimensional image of a ZSM-5 crystal (Si/Al~130) in the "triangular" strained state is shown its shape from several directions. The entire shape shows close resemblance to the scanning electron microscope (SEM) image of a crystal with more common (020) orientation from the same batch, shown in Fig. 1e.

The development of internal crystal strains, invisible to SEM, is the main focus of the present work. The inversion of the data to a complex density function also yields a real-space phase value for every point in space, which we illustrate as a color scale ranging from blue (–1 rad) to red (+1 rad). The phase is interpreted quantitatively as a projection onto the momentum transfer Q-vector of the local displacement of the crystal from an ideal undistorted lattice[4]. A phase of $\pi/2$ corresponds to a shift (along Q) of one quarter of (200) lattice spacing, or 0.25 nm. Figure 2 shows that the phase maps of the crystals from same batches intersecting through its centre as a function of temperature with different calcination conditions. The positive phase (red) indicates displacement along Q whereas the negative phase (blue) that in the opposite direction. In the crystals calcined at 450°C for 3 hours and 12 hours, initially unstrained, they begin to strain at 100°C and reach a maximum at 200°C. The maximum strain component is seen with a total phase excursion of 1.8 radians, corresponding to a total displacement of about 29 % of ZSM-5 (200) spacing, i.e., 0.29 nm. This means that the spatial derivative of displacement along the entire size (~2.0 μm) of the crystal is $\sim 10^{-4}$. In the image at 200°C, the edges of the sample are compressed but the centre part is expanded along Q || [200]. The deformation becomes smaller and more uniform with further increasing temperature. However, the crystals calcined at 550°C (independent of time) do not show strong displacement evolution. Note that the development of the "triangular" strained state upon heating was observed in almost all the crystals independent of crystal size, aluminum concentration, and the existence of copper atoms. Only the calcining temperature was found to affect this behavior.

Even though calcining at 450°C might leave a residue of the TPA inside the crystals, it is not clear how residual organic templates can give rise to the unusual and transient appearance of strained material inside the crystal. Therefore we first measured the existence of the organic template residue by element analysis (EA). The results in Table S1 show that ZSM-5 crystals calcined at 550°C do not contain any residual

TPA whereas those calcined at 450°C (independent of the calcination time) have minute amounts of nitrogen and carbon compounds. In order to find out where those residual organics locate, energy dispersive x-ray (EDX) spectroscopy and confocal fluorescence microscopy[25] were employed. In EDX measurements, the crystals calcined at 550°C and 450°C for 3 hours were found to contain residual organic template material. The relative atomic compositions measured at several positions of an individual crystal in Fig. S2 (a) calcined at 550°C and (b) calcined at 450°C are shown in Table S2 and S3, respectively. Among the composition of the organic templates, nitrogen was below the detection limit, but the carbon concentration was higher in the crystal calcined at 450°C. In that sample, the center part shows slightly higher concentration of carbon. Since the level of the absolute amount of carbon is very low, the distribution fluctuated from sample to sample.

Based on the observation above, fluorescence from organic templates (not completely decomposed) within ZSM-5 was measured by confocal fluorescence microscopy[25]. The fluorescence from the crystal calcined at 450 °C is displayed in Fig. S3(a) [also in Fig. 4d] in the range of 420-515 nm excited with a 405 nm laser. Because of very low concentration combined with the size of the crystal being close to the resolution limit, the fluorescence signal was very weak. The image obtained with 10 times of accumulations shows inhomogeneous density of organic materials, i.e., the centre part is higher than the outer part. From the sample calcined at 550°C, however, no fluorescence was detected. Description on S3(b) and (c) needed? NO!

To obtain the effect of organic templates to the thermal expansion behavior of ZSM-5, we applied high resolution x-ray powder diffraction (HRPD) to as synthesized ZSM-5 to compare the thermal expansion of calcined ZSM-5 (550°C for 12 hours and 450°C for 3 hours; curve A and B in Fig. 3, respectively) with as-synthesized material (before calcining; curve C). The part of HRPD data is shown in Fig. S4. The variation of lattice parameters of ZSM-5 along a-, b-, c-axis, and the unit cell volume are shown in Fig. 3a, 3b, 3c, and 3d (in vacuum), and 3e, 3f, 3g, and 3h (in nitrogen atmosphere), respectively. Differences in lattice parameter (Δd) are calculated with respect to the value of A at 25°C for each condition. Overall behavior of A and B are very similar, but C showed slope changes in thermal expansion. Along a-axis, the curve A exhibits negative thermal expansion while the curve C positive thermal expansion up to 300°C (in vacuum) and 250°C (in nitrogen) and negative thermal expansion thereafter. The lattice changes from curve B show similar behavior

as negative thermal expansion observed in A, but slightly positive thermal expansion is observed upto 150°C. Along b- and c-axis, thermal expansion behaviors for curve C do not show notable differences up to ~350°C in vacuum, whereas the slope changes from positive to negative at 250°C in nitrogen. Note that in nitrogen the values from curves A and C approach the same values at 400°C. It explains why "triangular" strain is released at 400°C, shown in Fig. 2.

All the information above allow us to model to simulate the strain pattern and resulting x-ray diffraction patterns using finite element analysis (FEA). Detail process is described in SI. We assume an inhomogeneous distribution of residual organic TPA template material within the crystal allowing the shape and area of distribution of residues, i.e., without giving any spatial constraints. The imaged phase $\varphi = \mathbf{Q}\cdot\mathbf{u}$ is only sensitive to the a-axis displacement at the (200) reflection used, which is the direction with opposite sign in thermal expansion of ZSM-5 before and after calcination. The center region, containing TPA, expands upon heating, while the border regions contract.

The FEA results in Fig. 4a-4c simulated for 200°C use effective thermal expansion coefficients derived from Fig. 3: α_a=-3.790×10^{-6} K^{-1}, α_b=3.392×10^{-6} K^{-1}, and α_c=-7.945×10^{-7} K^{-1} for the three principle axis directions of the sample after calcination at 550°C in nitrogen, and α_a=7.246^{-6} K^{-1}, α_b=2.572×10^{-6} K^{-1}, α_c=3.390×10^{-6} K^{-1} for those before calcination. The detailed thermal expansion coefficients are displayed in Table S4. We modeled the crystal with its actual dimensions rigidly bonded to a silicon substrate. Further information can be obtained in SI. The simulation we found which worked was based on inhomogeneities of the expansion coefficients, best illustrated by the "core-shell" structure in Fig. 4a. The spatial distribution of organic templates show a complete agreement with that obtained from the fluorescence mapping. It is also agreed with the fact that the core has a positive coefficient whereas the shell has negative expansion. From the calculation with the intrinsic negative thermal expansion of ZSM-5 and positive thermal expansion of silicon, shown in Fig. 4b, a gradual change in displacement is obtained along the crystal with no evidence of "triangular" deformation. Differential thermal expansion effects alone were unable to explain the observed structure. Because of the positive expansion of the substrate, calculations with other combination of thermal expansion coefficients shown in Fig. 4c did not obtain the observed displacement pattern. Figure 4d is the same image shown in Fig.

S3(a) expanded by 1.6 times for comparison.

Other possible scenarios for explaining the unique triangular shape of strain patterns could be inhomogeneous distribution of aluminum[26]. Evidence of variations of aluminum concentration between the rim and the center of the crystals has been found in our samples by x-ray microfluorescence experiments (see Fig. S5). This, together with the variation of the lattice parameter with aluminum content observed in ZSM-5[21] might give the core-shell structure hence a similar strain pattern. However, it should not be dependent on the calcination conditions because changes in the 200-300°C range are unlikely to be due to redistribution of aluminum atoms within the crystal. However, the strain could easily be explained by the organic template material, as in our model.

In this study, we have observed an internal deformation distribution of ZSM-5 zeolite microcrystals bonded to silicon substrates. The fully calcined crystals remain relaxed with a relatively small displacement field within the crystal, as resolved along the (200) Q-vector in our CDI method. While the distribution of residual organic impurities can be detected by other techniques, the strain field distribution inside the crystal due to such small traces was only possible to be detected by CDI. Before they are fully calcined, the crystals adopt a transient "triangular" strained state, maximally developed at 200°C, with a characteristic pattern of displacements, which can be attributed to a core-shell arrangement of strain with an inhomogeneous distribution of lattice parameter. The best model includes also the effects of differential expansion with respect to the substrate. This deformation propagates through the crystal to create a reversed pattern of displacements on the opposite side. The appearance of strain also depended on the starting state and temperature history in a way that is consistent with trapping of the organic TPA template material in the inner volume of the crystal. The macroscopic deformation seen in these small crystals affects adsorption and diffusion of molecules through the pores.

Methods Summary

Sample preparation. ZSM-5 crystals were synthesized by hydrothermal reaction from the gels consisting of tetraethyl orthosilicate (TEOS), sodium aluminate ($NaAlO_2$, 35% of Na_2O, and 35% of Al_2O_3), tetrapropylammonium hydroxide (TPAOH), and KOH. In order to obtain the crystals with different Si/Al ratio, the gels were composed of TEOS:$NaAlO_2$:TPAOH:H_2O = 7.0:0.28:1.0:600.0 for Si/Al~130 and TEOS:$NaAlO_2$:TPAOH:KOH:H_2O = 8.0:0.4:1.0:0.4:500.0 for Si/Al~60 or ~90. The gels were reacted at 180°C for 5 hours and 200°C for 24 hours in an autoclave for Si/Al~130 and Si/Al~60 to 90, respectively. The produced ZSM-5 crystals were isolated using centrifugation and subsequently washed with distilled deionized water several times. A colloidal solution, in which ZSM-5 crystals were dispersed in dilute solution of polyethylene imine dissolved in ethanol, was used for crystals to be isolated onto a silicon substrate. Subsequently, the samples were calcined at either at 450°C or 550°C for several hours in air. During the calcination, Si-O-Si chemical bonds were formed between the surface of zeolite and the Si substrate from terminal Si-OH groups by dehydration.

CDI experiments. Unfocussed coherent x-rays with wavelength of 0.1380 nm from the 34-ID-C beamline in the Advanced Photon Source, USA illuminated isolated samples mounted in a sample chamber in nitrogen environment with varying temperature. CXD patterns were measured with a charge-coupled device detector with 22.5 μm^2 pixels located about 2 m away from the sample. Three-dimensional diffraction data were collected as rocking curves of the sample tilt angle with steps of 0.01º or 0.016º with a total of 31 to 51 frames.

Confocal fluorescence microscopy. Fluorescence measurements were carried out witha confocal microscope (a Leica TCS SPE with a Leica DMI4000 B upright microscope) with 4 laser lines (405, 488, 532, and 635 nm). Emission spectra were measured in the range of 420-515, 505-555, 545-655, and 645-735 nm for 4 laser lines, respectively. Samples (ZSM-5 with dimension of 1.88 × 0.78 × 2.68 μm^3 and Silicalite-1 with 3.0 × 1.0 × 9.5 μm^3 along a-, b-, and c-axis of crystals, respectively) were placed on a cover glass and calcined before the measurements.

Thermal expansion of ZSM-5. The high resolution x-ray powder diffraction experiments in vacuum and in nitrogen atmosphere were performed at 9B beamline in the Pohang Light Source, Korea. The 20 × 1 mm^2 sized x-rays with the wavelength of 0.15494 nm or 0.15475 nm illuminated ZSM-5 as a function of temperature. The data was collected with multi detector system of seven detectors with analyzers located with installation angle of 20º. Because of high crystalline structure of ZSM-5, the diffraction was measured with the step size of 0.005º.

Finite Element Analysis (FEA). The COMSOL MULTIPHYSICS® package was used for FEA of the displacement along the different thermal expansion behavior in a ZSM-5 crystal. The ZSM-5 was modeled to have a core-shell structure with different thermal expansion coefficients measured by high resolution x-ray diffraction. In order to simplify the simulation, the rectangular parallelepiped with curved sides was used with same dimension measured by SEM, i.e., 1.88 × 0.78 × 2.68 μm^3 along a-, b-, and c-axis of ZSM-5, respectively.

REFERENCES

1. Davis, M. E. Ordered porous materials for emerging applications. *Nature* **417,** 813-821 (2002).
2. Smit, B. & Maesen, T. L. M. Towards a molecular understanding of shape selectivity. *Nature* **451**, 671-678 (2008).
3. Kärger, J. Single-file diffusion in zeolites. *Molecular Sieves – Science and Technology* **7**, 329-366 (2008).
4. Robinson, I. & Harder, R. Coherent X-ray diffraction imaging of strain at the nanoscale. *Nature Mater.* **8,** 291-298 (2009).
5. Park, S. H., Kunstleve, R. -W. G., Graetsch, H. & Gies, H. The thermal expansion of the zeolites MFI, AFI, DOH, DDR, and MTN in their calcined and as synthesized forms. *Stud. Surf. Sci. Catal.* **105**, 1989-1994 (1997).
6. Lai, Z. et al. Microstructural optimization of a zeolite membrane for organic vapor separation. *Science* **300**, 456-460 (2003).
7. Choi, J. et al. Grain boundary defect elimination in a zeolite membrane by rapid thermal processing. *Science* **325**, 590-593 (2009).
8. Pham, T. C. T., Kim, H. S. & Yoon, K. B. Growth of Uniformly Oriented Silica MFI and BEA Zeolite Films on Substrates. *Science* **334**, 1533-1538 (2011).
9. Lee, J. S., Lee, Y.-J., Tae, E. L., Park, Y. S. & Yoon, K. B. Synthesis of zeolite as ordered multicrystal arrays. *Science* **301**, 818-821 (2003).
10. Caro, J. & Noack, M. Zeolite Membranes - Status and Prospective, in *Advances in Nanoporous Materials*, Ernst, S. Ed. (Elsevier, Amsterdam, 2009), vol. 1, chap. 1, pp. 1-96.
11. Caro, J. & Noack, M. Zeolite membranes - Recent developments and progress. *Micropor. Mesopor. Mater.* **115**, 215-233 (2008).
12. O'Brien-Abraham, J. & Lin, J. Y. S. Zeolite Membrane Separations, in *Zeolites in industrial Separation and Catalysis*, Kulprathipanja, S. Ed. (Wiley VCH, Verlag, Weinheim, Germany, 2010), chap. 10, pp. 307-329.
13. O'Brien-Abraham, J., Kanezashi, M. & Lin, Y. S. Effects of adsorption-induced microstructural changes on separation on xylene isomers through MFI-type zeolite membranes. *J. Membr. Sci.* 320, 505-513 (2008).
14. Hedlund, J., Jareman, F., Bons, A.-J. & Anthonis, M. A masking technique

for high quality MFI membranes. *J. Membr. Sci.* 222, 163-179 (2003).

15. Bein, T. Synthesis and Applications of Molecular Sieve Layers and Membranes. *Chem. Mater. 8*, 1636-1653 (1996).
16. Jeong, H. -K., Lai, Z., Tsapatsis, M. & Hanson J. C. Strain of MFI crystals in membranes: An in situ synchrotron x-ray study. *Micropor. Mesopor. Mater.* **84,** 332-337 (2005).
17. Marinkovic, B. A. et al. Complex thermal expansion properties of Al-containing HZSM-5 zeolite: A x-ray diffraction, neutron diffraction and thermogravimetry study. *Micropor. Mesopor. Mater.* **111,** 110–116 (2008).
18. Chao, K.-J., Lin, J.-C., Wang, Y. & Lee, G. H. Single crystal structure refinement of TPA ZSM-5 zeolite. *Zeolites* **6**, 35-38 (1986).
19. Gao, X., Yeh, C. Y. & Angevine P. Mechanistic study of organic template removal from ZSM-5 precursors. *Micropor. Mesopor. Mater.* **70**, 27-35 (2004).
20. Gualtieri, M. L., Gualtieri, A. F. & Hedlund, J. The influence of heating rate on template removal in silicalite-1: An in situ HT-XRPD study. *Micropor. Mesopor. Mater.* **89**, 1-8 (2006).
21. Sen, S., Wusirika, R. R. & Youngman, R. E. High temperature thermal expansion behavior of H[Al]ZSM-5 zeolites: The role of Brønsted sites. *Micropor. Mesopor. Mater.* **87,** 217-223 (2006).
22. Pfeifer, M. A., Williams, G. J., Vartanyants, I. A., Harder. R. & Robinson, I. K. Three-dimensional mapping of a deformation field inside a nanocrystal. *Nature* **442,** 63-66 (2006).
23. Newton, M. C., Leake S. J., Harder R. & Robinson I. K. Three-dimensional imaging of strain in a single ZnO nanorod. *Nature Mater.* **9**, 120-124 (2010).
24. Fienup, J. R. Phase retrieval algorithms: a comparison. *Appl. Opt.* **21,** 2758-2769 (1982).
25. Karwacki, L. & Weckhuysen, B. M. New insight in the template decomposition process of large zeolite ZSM-5 crystals: an in situ UV-Vis/fluorescence micro-spectroscopy study. *Phys. Chem. Chem. Phys.* **13**, 3681-3685 (2011).
26. Ballmoos, R. & Meier, W. M. Zoned aluminium distribution in synthetic zeolite ZSM-5. *Nature* **289**, 782-783 (1981).

Corresponding author

Correspondence to: Hyunjung Kim

Contributions

H.K. supervised and coordinated all aspects of the project. ZSM-5 growth was carried out by N.C. J. and T. C. T. P. under the supervision of K.B.Y. Coherent X-ray diffraction measurements were carried out by W. C., S. S., H. P., R. H., I. K. R. , and H. K. CDI Data analysis was carried out by W. C. and R. H. Energy dispersive x-ray spectra measurements were done by T. C. T. P. Confocal fluorescence microscopy measurements were carried out by B. L. and W. C. under supervision of J. K. Powder diffraction measurements were carried out by W. C., S. S., H. P., and D. A. and data analysis done by W.C. H. P., and D. A. Finite element analysis calculation is carried out G. X., R. H. and W.C. under supervision of I.K.R and H. K. X-ray microfluorescence measurements were carried out by W.C., R. H., and I. M. W. C., K.B. Y., I.K.R., and H. K. wrote the paper. All authors discussed the results and commented on the manuscript.

ACKNOWLEDGMENTS
This research was supported by Basic Science Research Program through the National Research Foundation of Korea (NRF) funded by the Ministry of Education and the Ministry of Science, ICT & Future Planning (Nos. 2007-0053982, 2011-0012251, and R15-2008-006-01001-0), Sogang University Research Grant of 2012 and an ERC FP7 Advanced Grant 227711. W. C. was also supported by Hi Seoul Science/Humanities Fellowship from Seoul Scholarship Foundation. K.B.Y thanks the NRF project No. 2012M1A2A2671784. GX and IKR were supported by the "Nanoscupture" advanced grant from the European Research Council. Use of the Advanced Photon Source was supported by the US Department of Energy, Office of Science, Office of Basic Energy Science, under Contract No. DE-AC02-06CH11357.

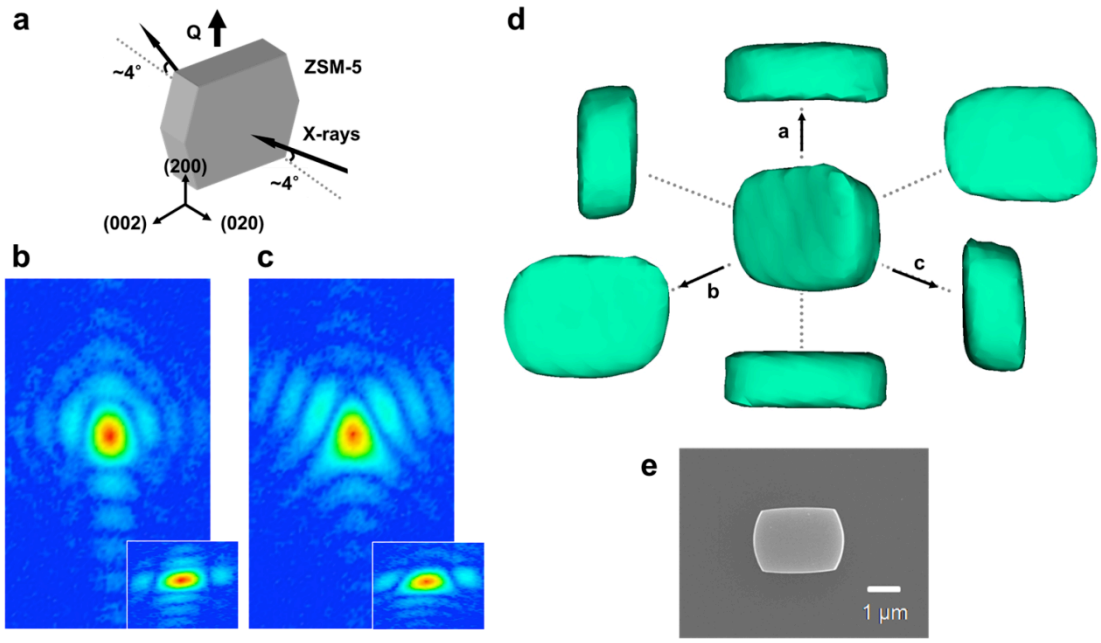

Figure 1 | CXD patterns and three-dimensional image of a ZSM-5 zeolite crystal. a, The geometry of a ZSM-5 zeolite microcrystal attached onto a silicon wafer in the CDI experiment. The momentum transfer wavevector Q for (200) Bragg reflection, determined by the direction of incident and scattered x-rays, is displayed. **b,** Diffraction pattern of a ZSM-5 crystal before heating measured by a CCD detector in the geometry shown in **a**. The inset pattern is perpendicular view of the three-dimensional pattern. **c,** The same crystal after heating to 200°C. **d,** Three-dimensional real-space image of the ZSM-5 microcrystal reconstructed from three-dimensional CXD patterns by the phase retrieval algorithm. The projected images parallel to a-, b-, and c-axis are shown. **e,** A typical scanning electron microscopy image of the sample along b-axis.

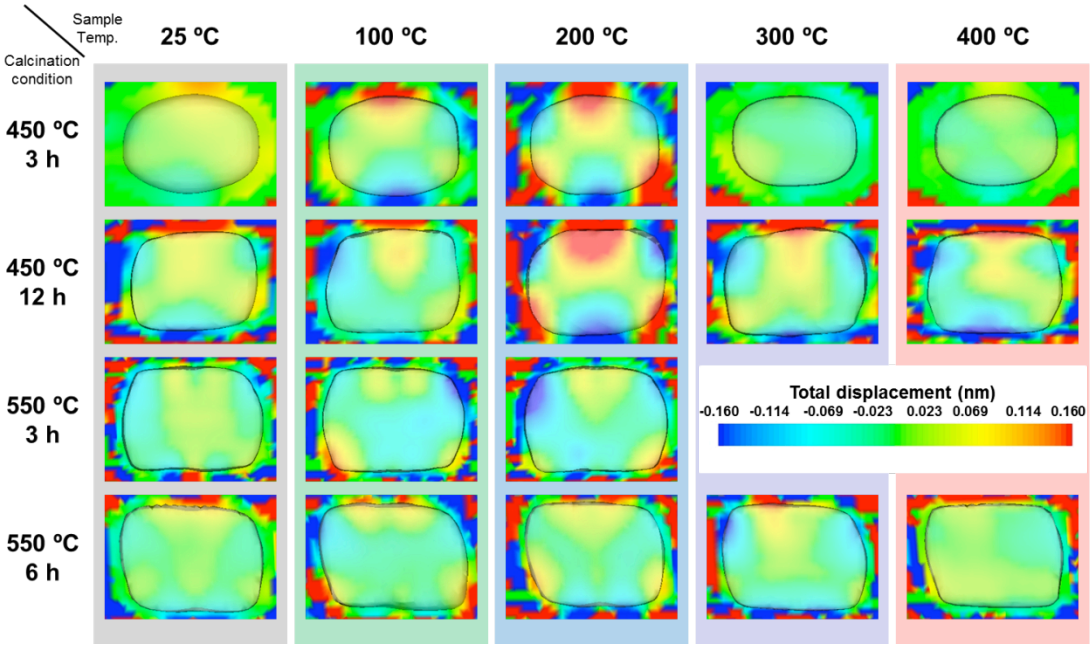

Figure 2 | Internal phase images depending on calcination condition as a function of temperature. Lattice displacement is shown as a map of phase, intersecting through the centre part of the crystals down their b-axis. The phase interpreted as the scalar product of the local deformation and the momentum transfer wavevector Q shows a dramatic change in the sample calcined at 450°C. The “triangular” pattern appears at 200°C and disappears with increasing temperature. However, this observation is not seen in the sample calcined at 550°C. The colour scale represents a range of ±1 radian corresponding to the displacement of ± 0.160 nm. Positive value (red) means the lattice moved to the same direction of Q whereas negative value (blue) in the opposite direction.

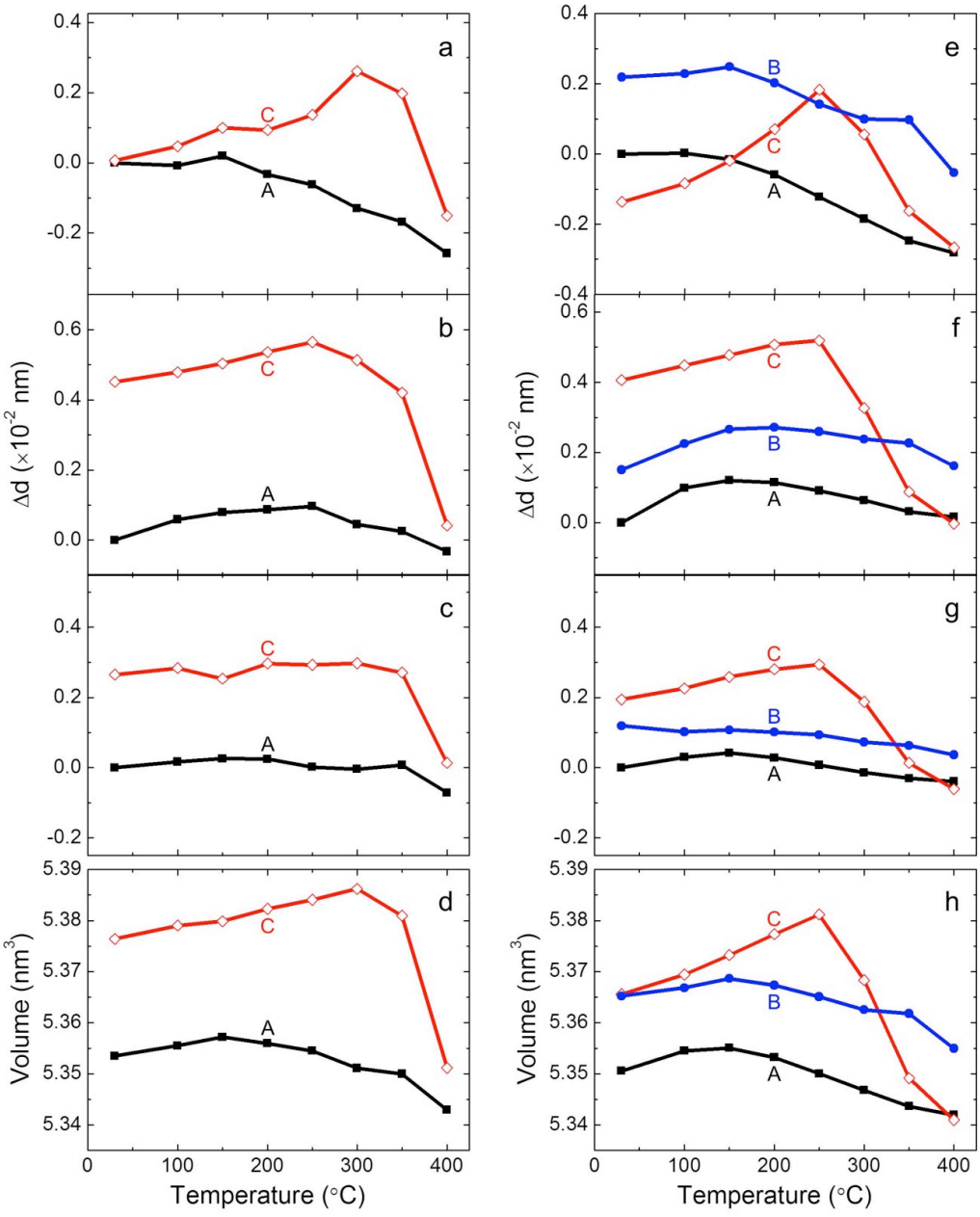

Figure 3 | Measured thermal expansion behavior of ZSM-5 calcined at 550°C (A), 450°C (B), and as-synthesized before calcination (C). The change of lattice parameters of ZSM-5 along a-, b-, c-axis and the volume of unit cell of ZSM-5 measured by high resolution powder diffraction experiments in vacuum are shown in **a**, **b**, **c**, and **d**, and in nitrogen atmosphere in **e**, **f**, **g**, and **h,** respectively. The lattice difference (Δd) is calculated by subtraction the value of A at 25°C from the measured value at each temperature.

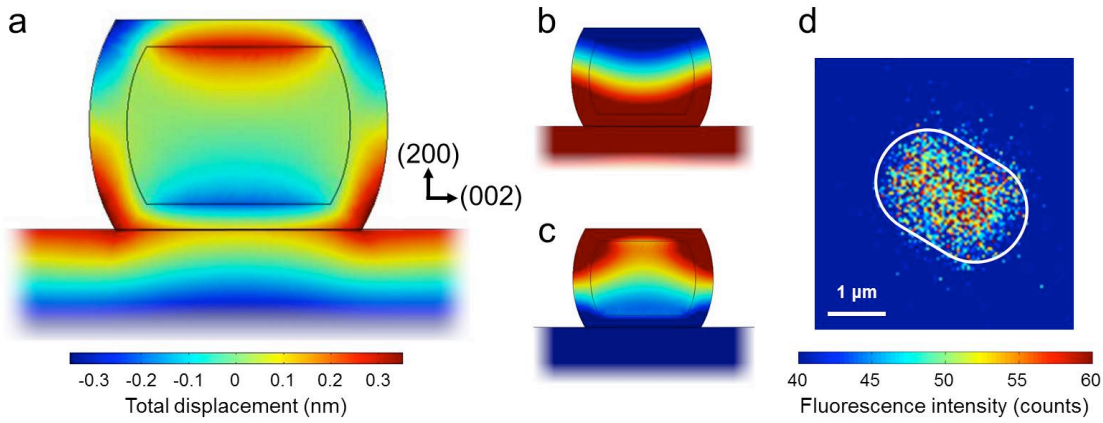

Figure 4 | FEA simulation of displacement distribution at 200°C with core-shell structure and confocal fluorescence microscope image.

a, The best model which produces the "triangular" displacement distribution. The calculation was set to have the positive thermal expansion coefficient of the core and negative thermal expansion coefficient of the shell. The magnitude of vertical displacement shown agrees with that measured by CDI in Fig. 2. The colour in scale bar indicates amount of total displacement in nanometer scale. Positive value shown in red means the point moves up while negative value does the point moves down. **b,** The result due to the known intrinsic negative thermal expansion behavior of ZSM-5 attached to a silicon substrate exhibits a gradual pattern, which does not agree with our experimental result. **c,** Same as model **a** with exchanged thermal expansion coefficients of the core and the shell, the resultant pattern does not agree with observation. **d,** Localized residual templates detected with a confocal fluorescence microscope. Fluorescence in the range of 420-515 nm excited with a laser with 405 nm of wavelength shows inhomogeneous distribution which allows modeling with FEA. White solid line indicates the edge of the crystal and rainbow coloured scale bar fluorescence intensity. Details are in SI.